Systematical study of thermal width of heavy quarkonia in a finite temperature magnetized background from holography

Sheng-Qin Feng,[1,2,*] Yan-Qing Zhao,[1] and Xun Chen[2]

[1]*College of Science, China Three Gorges University, Yichang 443002, China*
[2]*Key Laboratory of Quark and Lepton Physics (Ministry of Education) and Institute of Particle Physics, Central China Normal University, Wuhan 430079, China*

(Received 14 October 2019; published 31 January 2020)

By simulating the finite temperature magnetized background at the Relativistic Heavy Ion Collider and LHC energies, we systematically study the characteristics of the thermal width and potential of heavy quarkonia. It is found that the magnetic field has less influence on the real potential but has a significant influence on the imaginary potential, especially in the low deconfined temperature. Extracted from the effect of thermal worldsheet fluctuations about the classical configuration, the thermal width of $\Upsilon(1S)$ at the finite temperature magnetized background is investigated. It is found that at the low deconfined temperature the magnetic field can generate a significant thermal fluctuation of the thermal width of $\Upsilon(1S)$, but with the increase of temperature, the effect of magnetic field on the thermal width becomes less important, which means the effect of high temperature completely exceeds that of magnetic field and magnetic field becomes less important at high temperature. The thermal width decreases with the increasing rapidity at the finite temperature magnetized background. It is also observed that the effect of the magnetic field on the thermal width when the dipole is moving perpendicular to the magnetic field is larger than that moving parallel to the magnetic field at $T_c < T < 1.5T_c$, which implies that the magnetic field tends to enhance thermal fluctuation when the dipole is moving perpendicular to magnetic field, but when $T > 2T_c$, the effect of magnetic field on the thermal fluctuation is almost the same whether dipole moving perpendicular or parallel to the magnetic field.

DOI: 10.1103/PhysRevD.101.026023

I. INTRODUCTION

A new state of matter, so-called quark-gluon plasma (QGP), has been generated in relativistic heavy-ion collisions at the Relativistic Heavy Ion Collider (RHIC) and the LHC [1–3]. The heavy quarkonia (J/Ψ and Υ mainly) are formed in hard processes before the thermalization of the plasma, which are taken as useful probes to study the formation and evolution of the QGP [4]. The well-known work of Matsui and Satz [5] argued that the binding interaction of the heavy quark-antiquark ($Q\bar{Q}$) pair in a thermal bath is screened by the medium, resulting in the melting of the heavy quarkonia. In the study of heavy-ion collisions, besides high temperature, another important finding is the generation of a strong magnetic field of noncentral heavy-ion collisions at the RHIC and the LHC [6–13]. Since the magnetic field in relativistic heavy-ion collisions is so great, people believe that the strong magnetic fields can provide some deep investigations of the dynamics of QCD.

The interaction energy $V_{Q\bar{Q}}$ of the $Q\bar{Q}$ pair may possess a finite imaginary part $\mathrm{Im}V_{Q\bar{Q}}$, which can be used to calculate a thermal width of the quarkonium at finite temperature [14–17]. The calculations of $\mathrm{Im}V_{Q\bar{Q}}$ related to heavy-ion collisions in QCD have been carried out for static $Q\bar{Q}$ pairs by using lattice QCD [18–20] and perturbative QCD [14]. The dissociation of quarkonia is one of the most important experimental signals for QGP formation. Some publications argued [21–24] that the imaginary part of the potential $\mathrm{Im}V_{Q\bar{Q}}$ may be an important reason responsible for this suppression rather than color screening. The imaginary potential has been subsequently studied in weakly coupled theories by Refs. [18,25]. However, an available method of the imaginary potential in recent years [14,26,27] has been used in strongly coupled theories with the aid of nonperturbative methods of anti-de Sitter (AdS)/QCD.

*fengsq@ctgu.edu.cn

The imaginary potential of quarkonia for $\mathcal{N}=4$ super Yang-Mills theory was studied by Noronha and Dumitru in their seminal work [28]. This imaginary contribution originates from thermal fluctuations around the bottom of the classical sagging string in the bulk that links the heavy quarks situated at the boundary in the dual gravity picture. The imaginary potential $\mathrm{Im}V_{Q\bar{Q}}$ related to the effect of thermal fluctuations is due to the interactions between the heavy quarkonia and the medium. Subsequently, a large number of research work about $\mathrm{Im}V_{Q\bar{Q}}$ was carried out with gauge/gravity duality. For instance, the $\mathrm{Im}V_{Q\bar{Q}}$ of static quarkonia was studied in Refs. [29,30]. References [31,32] studied the effect of moving quarkonia on $\mathrm{Im}V_{Q\bar{Q}}$. The influences of chemical potential and magnetic field on $\mathrm{Im}V_{Q\bar{Q}}$ were investigated in Refs. [33,34]. The studies of $\mathrm{Im}V_{Q\bar{Q}}$ in some AdS/QCD models are provided in Refs. [35,36].

On the other hand, strong magnetic field plays an essential role in noncentral heavy-ion collisions at the RHIC and LHC [6–13]. Strong magnetic field also provides a good probe of the dynamics of QCD. To accurately determine the suppression of quarkonia formed in relativistic heavy-ion collisions, it is necessary to evaluate the thermal width of $\Upsilon(1S)$ for moving quarkonia in the finite temperature magnetized QGP background at the RHIC and LHC energies. Reference [37] studies the charmonium dissociation in a strongly coupled chiral plasma in the presence of magnetic field and axial charge imbalance. This type of plasma carries anomalous flow induced by the chiral anomaly and exhibits novel transport phenomena such as chiral magnetic effect. It is expected that a charmonium dissociation induced by the chiral anomaly in heavy-ion collisions becomes possible.

Reference [38] computed the momentum dependence of meson widths within the gauge/gravity duality. It was proposed that the thermal width becomes very large for the rapidly moving meson, and the imaginary part of rapidly moving mesons may be already large enough to cause suppression of these states in a strongly coupled plasma even before complete dissociation. Thus, Refs. [39–41] indicate that the dissociation temperature of the meson decreased with the pair's rapidity. By simulating the background of finite temperature magnetized background at the RHIC and LHC energies, we restrict ourselves to the range of temperature and magnetic field corresponding to RHIC and LHC energies to study the potential and thermal width for the dipole moving parallel and pedicular to the magnetic field. This paper is organized as follows. In Sec. II, we introduce the setup of the gravity background with backreaction of magnetic field through the Einstein-Maxwell (EM) system. These cases in which the $Q\bar{Q}$ dipole moving parallel and perpendicular to the direction of the magnetic field are discussed in Secs. III and IV, respectively. In Sec. V, we make a comparison of the results of dipole moving parallel and perpendicular to the magnetic field direction. And then we make conclusions in Sec. VI.

II. SETUP

The action of the gravity background with backreaction of magnetic field through the EM system [42–44] is given as

$$S=\frac{1}{16\pi G_5}\int \mathrm{d}x^5\sqrt{-g}\left(R-F^{MN}F_{MN}+\frac{12}{L^2}\right), \quad (1)$$

where R is the scalar curvature, G_5 is the $5D$ Newton constant, g is the determinant of metric $g_{\mu\nu}$, L is the AdS radius, and F_{MN} is the U(1) gauge field [44].

The Einstein equation for the EM system could be derived as

$$E_{MN}-\frac{6}{L^2}g_{MN}-2\left(g^{IJ}F_{MJ}F_{NJ}-\frac{1}{4}F_{IJ}F^{IJ}g_{MN}\right)=0, \quad (2)$$

where $E_{MN}=R_{MN}-\frac{1}{2}Rg_{MN}$, R_{MN} and R are the Einstein tensor, the Ricci tensor, and Ricci scalar, respectively. The ansatz of metric originally came from Refs. [45,46],

$$ds^2=\frac{R^2}{z^2}\left[-f(z)dt^2+h(z)(dx_1^2+dx_2^2)+q(z)dx_3^2+\frac{dz^2}{f(z)}\right], \quad (3)$$

where $f(z=z_h)=0$ is located at horizon $z=z_h$ and $q(z)$ together with $h(z)$ is a regular function of z for $0\le z\le z_h$. The specific equations of motion derived from the action and the perturbative solution of $f(z)$, $h(z)$, and $q(z)$ have been discussed by Refs. [44,47]. Using the $r=\frac{L^2}{z}$ $(L=1)$, we can derive a metric with r as follows:

$$ds^2=r^2(-f(r)dt^2+h(r)(dx_1^2+dx_2^2)+q(r)dx_3^2)+\frac{1}{r^2f(r)}dr^2. \quad (4)$$

For a first-order approximation, one can take the leading expansion in Refs. [44,47] as

$$f(r)=1-\frac{r_h^4}{r^4}\left(1-\frac{2B^2}{3r_h^4}\log\left(\frac{r_h}{r}\right)\right), \quad (5)$$

$$q(r)=1+\frac{2}{3}B^2\log\left(\frac{1}{r}\right)\frac{1}{r^4}, \quad (6)$$

$$h(r)=1-\frac{1}{3}B^2\log\left(\frac{1}{r}\right)\frac{1}{r^4}. \quad (7)$$

Notice that B is related to the physical magnetic field $\mathfrak{B}$ at the boundary by the equation $\mathfrak{B} = \sqrt{3}B$, and z_h is the horizon of the black hole. If we take $B \leq 0.15\ \mathrm{GeV}^2$, the corresponding physical magnetic field is $\mathfrak{B} \leq 0.26\ \mathrm{GeV}^2$, which conforms to the magnitude of real magnetic field generated by at the RHIC and LHC energies. The Hawking temperature with magnetic field B is computed as

$$T(r_h, B) = \frac{r_h}{\pi} - \frac{B^2}{6\pi r_h^3}, \tag{8}$$

where $T(r_h, B)$ is a function of the position of the horizon and the magnetic field corresponds to the temperature of the thermal bath in the gauge theory. At the end of the setup, it is necessary to check the validity of the first-order perturbative solutions of $f(r)$, $h(r)$, and $q(r)$ in Eqs. (5), (6), and (7). It was pointed out [42] that the perturbative solution can work well only when $B \ll T^2$. After inserting the temperature and magnetic field into the IR expansion, Refs. [44,47] made some comparisons of the leading, next-leading, and next-next-leading order of these perturbative solutions and found that the approximations of leading order Eqs. (5), (6) and (7) are good enough for $T \geq 0.15$ GeV and $B \leq 0.15\ \mathrm{GeV}^2$. In the paper, the corresponding temperature range and magnetic field range are chosen as $0.15\ \mathrm{GeV} \leq T \leq 0.6\ \mathrm{GeV}$ and $0.02\ \mathrm{GeV}^2 \leq B \leq 0.15\ \mathrm{GeV}^2$, which conforms to the range of temperature and magnetic field at the RHIC and LHC erergies.

III. DIPOLE MOVING PARALLEL TO THE MAGNETIC FEILD

In the section, we assume that the initial state of $Q\bar{Q}$ is oriented in the direction of magnetic field and the magnetic field direction is along the x_3 axis. A reference frame in which the plasma is at rest and the $Q\bar{Q}$ dipole is moving with a constant rapidity is chosen, and one can boost to a reference frame in which the dipole is at rest but the plasma is moving past it. We can utilize this fact to study the effect of the plasma on a $Q\bar{Q}$ pair in the thermal medium. By considering the plasma is at rest, one can boost our frame in one direction with rapidity β.

When the heavy quark is moving parallel to the magnetic field along the x_3 direction with rapidity β, the coordinates are parametrized by

$$\mathrm{d}t = \mathrm{d}t' \cosh\beta - \mathrm{d}x_3' \sinh\beta, \tag{9}$$

$$\mathrm{d}x_3 = -\mathrm{d}t' \sinh\beta + \mathrm{d}x_3' \cosh\beta. \tag{10}$$

Substituting (9) and (10) into the metric (4), one can obtain

$$\begin{aligned} ds^2 = {} & (-r^2 f(r)\cosh^2\beta + r^2 q(r)\sinh^2\beta)dt^2 \\ & - 2\sinh\beta\cosh\beta(r^2 q(r) - r^2 f(r))dtdx_3 \\ & + (-r^2 f(r)\sinh^2\beta + r^2 q(r)\cosh^2\beta)dx_3^2 \\ & + r^2 h(r)(dx_1^2 + dx_2^2) + \frac{1}{r^2 f(r)}dr^2. \end{aligned} \tag{11}$$

By considering the dipole moving parallel to the wind, one can take

$$t = \tau, \qquad x_1 = x_2 = 0, \qquad x_3 = \sigma, \qquad r = r(\sigma). \tag{12}$$

Then, the metric is given as

$$\begin{aligned} ds^2 = {} & (-r^2 f(r)\cosh^2\beta + r^2 q(r)\sinh^2\beta)d\tau^2 \\ & - 2\sinh\beta\cosh\beta(r^2 q(r) - r^2 f(r))d\tau d\sigma \\ & + \left(-r^2 f(r)\sinh^2\beta + r^2 q(r)\cosh^2\beta + \frac{\dot{r}^2}{r^2 f(r)}\right)d\sigma^2. \end{aligned} \tag{13}$$

Holographically, in the supergravity limit which corresponds to a strongly coupled plasma, one can evaluate the expectation value of the Wilson loop $W(C)$ by the prescription

$$\langle W(C)\rangle \sim e^{-iS_{NG}}, \tag{14}$$

where S_{NG} is the classical Nambu-Goto action of a string in the bulk, which can be given as

$$S_{NG} = -\frac{1}{2\pi\alpha'}\int \mathrm{d}\sigma d\tau \sqrt{-\det g_{ab}}, \tag{15}$$

where the induced metric of the worldsheet g_{ab} is given by

$$g_{ab} = g_{MN}\partial_a X^M \partial_b X^N, \qquad a, b = 0, 1, \tag{16}$$

evaluated at an extremum of the action, $\delta S_{NG} = 0$. The string worldsheet coordinates are given in static gauge, $X^\mu = (t, x_3, 0, 0, r(x_3))$, $\tau = t$, and $\sigma = x_3$ for the rectangular Wilson loop.

If the quark and antiquark are located at $x_3 = L/2$ and $x_3 = -L/2$, respectively, the rectangular Wilson loop of spatial length L and time extension $\mathcal{T}$ are studied. Plugging S_{NG} back in (14), one can evaluate the real part of $V_{Q\bar{Q}}$. By considering thermal fluctuations of the string, one will be able to evaluate the imaginary part of $V_{Q\bar{Q}}$. With the metric of (13), the Nambu-Goto action (15) can be calculated as

$$S_{NG} = \frac{\mathcal{T}}{2\pi\alpha'}\int_{-L/2}^{L/2} \mathrm{d}x_3 \sqrt{a(r) + b(r)\dot{r}^2}. \tag{17}$$

The Lagrangian density is taken as

$$\mathcal{L} = \sqrt{a(r) + b(r)\dot{r}^2}, \tag{18}$$

with

$$a(r) = r^4 f(r) q(r), \tag{19}$$

and

$$b(r) = \cosh^2\beta - \frac{q(r)}{f(r)}\sinh^2(\beta). \tag{20}$$

Note that the Lagrangian density does not depend on x_3 explicitly; then, a conserved quantity can be given as

$$\mathcal{L} - \frac{\partial \mathcal{L}}{\partial \dot{r}}\dot{r} = \text{constant}. \tag{21}$$

The boundary condition at $x_3 = 0$, when $r = r_c$, $\dot{r}_c = dr/dx_3|_{r=r_c} = 0$. From above, we can derive

$$\dot{r} = \sqrt{\frac{a(r)^2 - a(r_c)a(r)}{a(r_c)b(r)}}. \tag{22}$$

The distance of the heavy $Q\bar{Q}$ pair can be calculated as

$$L = 2\int_{r_c}^{\infty} dr \sqrt{\frac{a(r_c)b(r)}{a(r)^2 - a(r_c)a(r)}}. \tag{23}$$

The real part of the heavy-quark potential can be derived as

$$\mathrm{Re}V_{Q\bar{Q}} = \frac{1}{\pi\alpha'}\int_{r_c}^{\infty} dr\left(\sqrt{\frac{a(r)b(r)}{a(r) - a(r_c)}} - \sqrt{b_0(r)}\right) - \frac{1}{\pi\alpha'}\int_{r_h}^{r_c} dr\sqrt{b_0(r)}, \tag{24}$$

where $b_0(r) = b(r \to \infty)$.

The real part of the heavy-quark potential as (24) can be computed by using the classical solution to the Nambu-Goto action (17). To explore $\mathrm{Im}V_{Q\bar{Q}}$, we have to consider the effect of thermal worldsheet fluctuations of the classical configuration $r = r_c(x_3)$. Although such fluctuations should be small, they may turn the integrand of (17) negative near $x_3 = 0$ and create an imaginary part for the effective string action. The corresponding physical picture is that some part of the string may reach the horizon through thermal fluctuations shown in Fig 1. If the bottom of the classical string solution is close enough to the horizon, thermal worldsheet fluctuations of very long wavelength may be able to reach the black brane horizon.

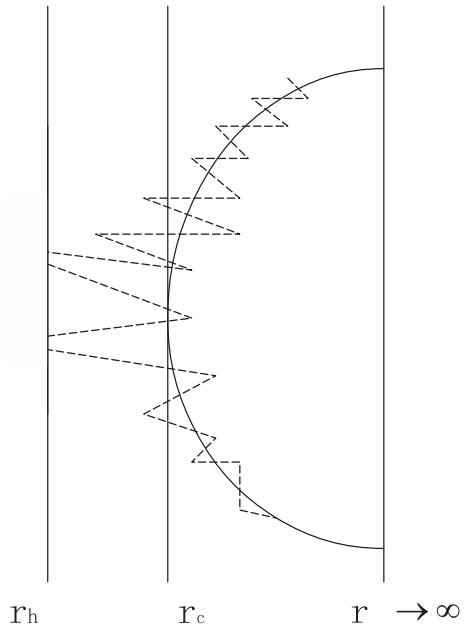

FIG. 1. An illustration of the effect of thermal fluctuations around the classical string configuration (solid line). The dashed line is for thermal fluctuations.

It is well known that an imaginary potential $\mathrm{Im}V_{Q\bar{Q}}$ is an imaginary part of the potential, which can be used to define a thermal decay width. For weak coupling, the thermal width is associated with the imaginary part of the gluon self-energy induced by Landau damping and the $Q\bar{Q}$ color singlet-to-octet thermal breakup. In this approach, the thermal width of heavy-quarkonium states comes from the effect of the thermal fluctuation due to the interactions between the heavy quarks and the strongly coupled medium. By considering the thermal worldsheet fluctuations about classical configuration, one can extract the imaginary potential and thermal width; the detailed analysis can be found in Refs. [29,30]. The imaginary potential is given as

$$\mathrm{Im}V_{Q\bar{Q}} = -\frac{1}{2\sqrt{2}\alpha'}\left(\frac{\sqrt{a'(r_c)}}{2a''(r_c)} - \frac{a(r_c)}{a'(r_c)}\right)\sqrt{b_0(r)}, \tag{25}$$

where $a'(r_c)$ and $a''(r_c)$ are the values of the first and second derivatives of $a(r)$ to r at r_c, respectively.

As follows, we will use a first-order nonrelativistic expansion [29] to estimate the thermal width $\Gamma_{Q\bar{Q}}$ of the heavy quarkonia,

$$\Gamma_{Q\bar{Q}} = -\langle\psi|\mathrm{Im}V_{Q\bar{Q}}(L,T)|\psi\rangle, \tag{26}$$

where

$$\langle\vec{r}|\psi\rangle = \frac{1}{\sqrt{\pi}a_0^{3/2}}e^{-r/a_0} \tag{27}$$

is the ground-state wave function of a particle in a Coulomb-like potential $V(L) = -K/L$, where the Bohr radius is defined as $a_0 = 2/(m_Q K)$ and m_Q is the mass of the heavy quark Q. For the $\Upsilon(1S)$ state, the thermal width is given as

$$\frac{\Gamma_{Q\bar{Q}}}{T} = -\frac{4}{Ta_0}\int_0^\infty d\omega e^{-\frac{2\omega}{Ta_0}}\omega^2 \frac{\mathrm{Im}V_{Q\bar{Q}}}{T}(\omega), \tag{28}$$

where $a_0 \sim 0.6$ GeV^{-1} and $m_Q = 4.6$ GeV for the calculation of $\Upsilon(1S)$ thermal width. Note that the imaginary potential is defined in the region $(L_{\min}, L_{\max})$ instead of taking the integral from zero to infinity, which means the imaginary potential starts at $L_{\min}$, which can be computed by solving $\mathrm{Im}V_{Q\bar{Q}} = 0$ and ends at a $L_{\max}$. The solution is called a conservative approach [48].

IV. DIPOLE MOVING PERPENDICULAR TO THE MAGNETIC FEILD

In this section, we assume that the initial state of $Q\bar{Q}$ is oriented transverse to the direction of magnetic field, and the magnetic field direction is along the x_3 axis. By considering the system moves along the x_1 direction with rapidity β, one can take

$$t = \tau, \quad x_2 = x_3 = 0, \quad x_1 = \sigma, \quad r = r(\sigma). \tag{29}$$

Then, the metric of dipole moving perpendicular to the magnetic field becomes

$$\begin{aligned} ds^2 = {} & (-r^2 f(r)\cosh^2\beta + r^2 h(r)\sinh^2\beta)d\tau^2 \\ & - 2\sinh\beta\cosh\beta(r^2 h(r) - r^2 f(r))d\tau d\sigma \\ & + \left(-r^2 f(r)\sinh^2\beta + r^2 h(r)\cosh^2\beta + \frac{\dot{r}^2}{r^2 f(r)}\right)d\sigma^2. \end{aligned} \tag{30}$$

The Lagrangian density is

$$\mathcal{L}_P = \sqrt{a_P(r) + b_P(r)\dot{r}^2}, \tag{31}$$

where

$$a_P(r) = r^4 f(r)h(r), \tag{32}$$

and

$$b_P(r) = \cosh^2\beta - \frac{h(r)}{f(r)}\sinh^2(\beta). \tag{33}$$

The real part of the heavy-quark potential can be calculated as

$$\begin{aligned} \mathrm{Re}V_{Q\bar{Q}} = {} & \frac{1}{\pi\alpha'}\int_{r_c}^\infty dr\left(\sqrt{\frac{a_P(r)b_P(r)}{a_P(r) - a_P(r_c)}} - \sqrt{b_{P0}(r)}\right) \\ & - \frac{1}{\pi\alpha'}\int_{r_h}^{r_c} dr\sqrt{b_{P0}(r)}. \end{aligned} \tag{34}$$

where $b_{P0}(r) = b_P(r \to \infty)$.

Similarly, one can calculate the imaginary part of the heavy-quark potential when dipole moves perpendicular to the magnetic field,

$$\mathrm{Im}V_{Q\bar{Q}} = -\frac{1}{2\sqrt{2}\alpha'}\left(\frac{\sqrt{a_P'(r_c)}}{2a_P''(r_c)} - \frac{a_P(r_c)}{a_P'(r_c)}\right)\sqrt{b_{P0}(r)}. \tag{35}$$

V. COMPARISON OF DIPOLE MOVING PARALLEL AND PERPENDICULAR TO THE MAGNETIC FIELD

To study the effects of the magnetic field on the imaginary potential and $\Upsilon(1S)$ thermal distributions in the finite temperature magnetized background, we make a comparison of the dipole moving parallel and perpendicular to the magnetic fields cases. As we know, the $Q\bar{Q}$ pair is not generated in the static QGP medium but in a moving QGP medium. Therefore, we should consider the influence of the moving QGP medium on the $Q\bar{Q}$ pair. To study quarkonia thermal features in RHIC and LHC energies, we choose some special magnetic fields $B = 0.02$ GeV^2, $B = 0.15$ GeV^2 and with temperatures as $T = 0.15$, 0.25, and 0.33 GeV in RHIC and LHC energies. Figure 2 publishes the behavior of LT as a function of $y_c = r_h/r_c$ for different magnetic fields B with different

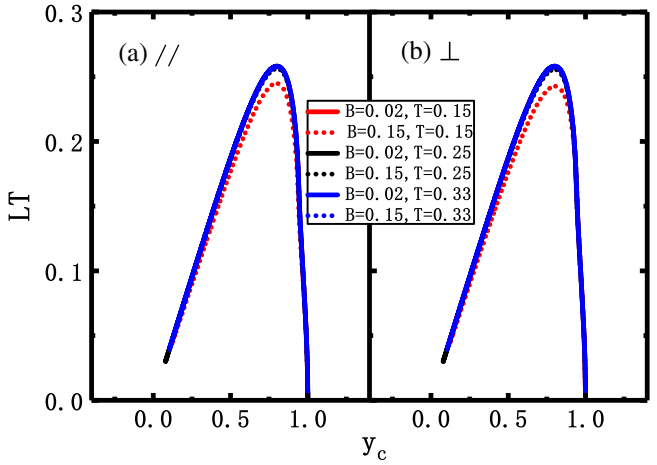

FIG. 2. LT vs y_c when dipole moves parallel and perpendicular to the magnetic fields for different temperatures and magnetic fields at fixed moving rapidity($\beta = 0.5$). Figures 2(a)and 2(b) are for the case of a dipole moving parallel and perpendicular to the magnetic field, respectively. The solid line is for $B = 0.02$ GeV^2, and the dashed line is for $B = 0.15$ GeV^2.

temperatures. It is found that the magnetic field has a significant effect on the relationship between LT and y_c at the low deconfined temperature ($T_c = 0.15$ GeV). But with the increase of temperature $T > T_c$, the influence of the magnetic field on the relationship between LT and y_c becomes less and less important when the dipole is moving both parallel and perpendicular to the magnetic field. There is a maximum value of LT located at $y_{c,\max}$, when $y < y_{c,\max}$, and LT is an increasing function of y_c, but when $y > y_{c,\max}$, LT is a decreasing function of y_c.

The maximum value of LT ($LT_{\max}$), which defines a dissociation length for $Q\bar{Q}$ [39,40], as a function of magnetic field B has been studied in Fig. 3. Figure 3 illustrates that increasing B reduces $LT_{\max}$ for the moving $Q\bar{Q}$. It is found that the magnetic field has a significant effect on the dissociation length for $Q\bar{Q}$ at the low deconfined temperature T_c; however, with the increase of temperature, the effect of magnetic field on dissociation length $LT_{\max}$ become less and less significant. When the temperature reaches 0.33 GeV, $LT_{\max}$ remains unchanged with the increase of magnetic field. In this case, the dominant configuration for S_{NG} should be two straight strings running from the boundary to the horizon. Moreover, the dissociation properties of heavy quarkonia should be sensitive to the imaginary part of the potential.

Figures 4(a) and 4(b) include comparisons of the real potential of $Q\bar{Q}$ pair vs LT for a dipole moving parallel and perpendicular to the magnetic field, respectively. Generally speaking, the difference of the effects of dipole moving parallel and perpendicular to magnetic fields on the relationship between real potential and LT is not very obvious. From Figs. 4(a) and 4(b), we find out that no matter how the magnetic field or temperature changes the real potential remains unchanged at the RHIC and LHC energies.

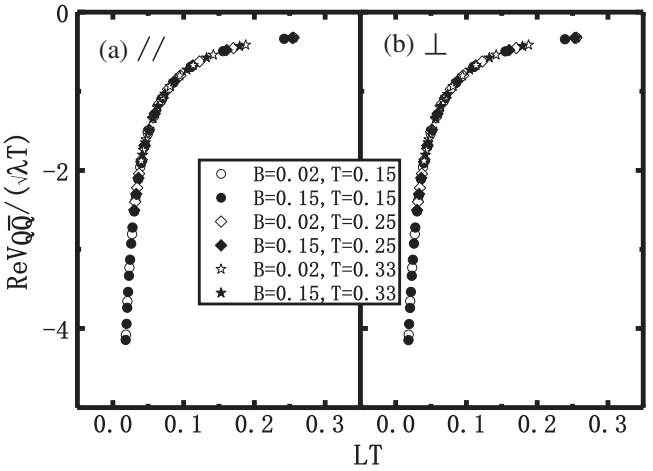

FIG. 4. The real potential of quark-antiquark pair vs LT with different magnetic fields and temperatures for dipole moving parallel (a) and perpendicular (b) to magnetic field, respectively.

As shown in Figs. 5(a) and 5(b), the imaginary potential starts at a $L_{\min}$, which can be computed by solving $\mathrm{Im}V_{Q\bar{Q}} = 0$, and ends at a $L_{\max}$. We also find that at the low deconfined temperature ($T = T_c = 0.15$ GeV) increasing the magnetic field leads to an increase of the absolute value of the imaginary potential and makes the imaginary potential $\mathrm{Im}V_{Q\bar{Q}}$ occur at a smaller interquark distance. When the temperature increases to $T = 0.33$ GeV, the effect of the magnetic field on $\mathrm{Im}V_{Q\bar{Q}}$ becomes less and less important. Comparing Fig. 5(a) with Fig. 5(b), we find that the absolute value of the imaginary potential in the case of the dipole moving parallel to the magnetic field is apparently bigger than the case of the dipole moving perpendicular to the magnetic field.

Figure 6 shows the thermal width of the $\Upsilon(1S)$ with nonzero magnetic fields at different finite temperatures for

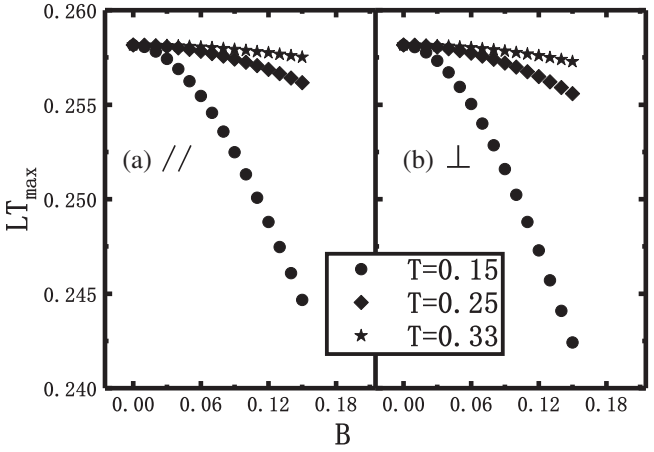

FIG. 3. The dependencies of maximum value of LT ($LT_{\max}$) on magnetic field B with different temperatures for dipole moving parallel (a) and perpendicular (b) to the magnetic field direction, respectively.

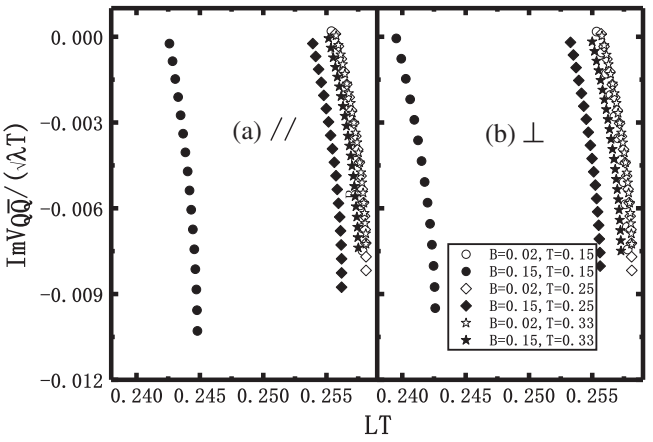

FIG. 5. The imaginary potential $\mathrm{Im}V_{Q\bar{Q}}$ of the quark-antiquark pair vs LT with different magnetic field and temperatures. Figure 5(a) is for the dipole moving parallel to the magnetic field and Fig. 5(b) is for perpendicular to the magnetic field.

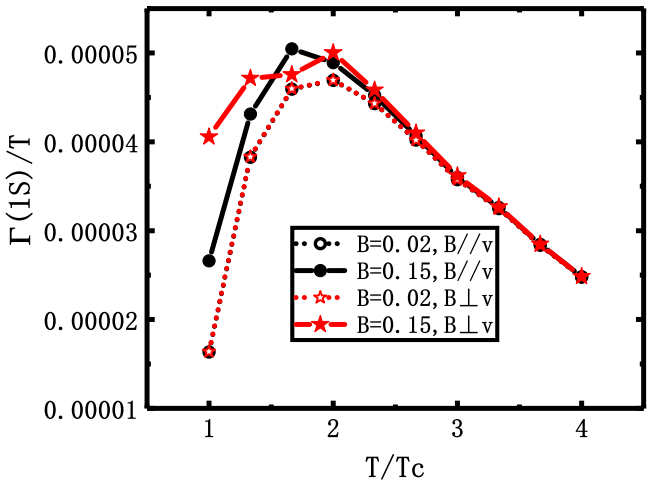

FIG. 6. The thermal width $\Gamma_{Q\bar{Q}}$ of the $\Upsilon(1S)$ state divided by the temperature T vs T/T_c under different magnetic fields for the dipole moving parallel and perpendicular to the magnetic field, respectively. The fixed rapidity is given as $\beta = 0.5$.

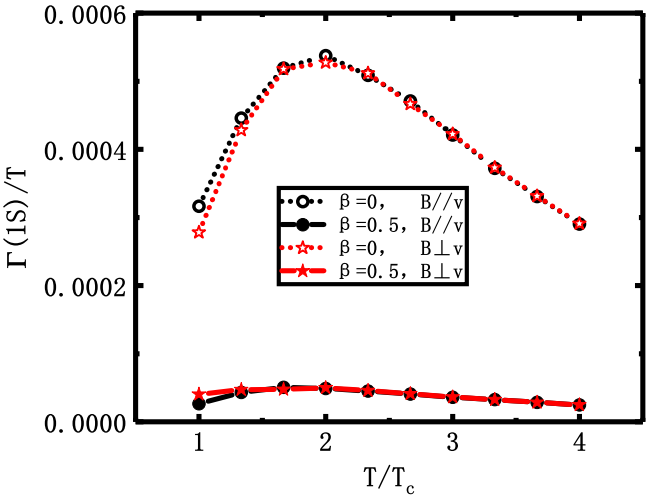

FIG. 7. The thermal width $\Gamma_{Q\bar{Q}}$ of the $\Upsilon(1S)$ state divided by the temperature T vs T/T_c under different rapidities for the dipole moving parallel and perpendicular to the magnetic field, respectively. The fixed magnetic field is given as $B = 0.15$ GeV^2.

the dipole moving parallel and perpendicular to the magnetic field case. We find some interesting characteristics of the thermal width varying with the magnetic field and temperature:

(1) Increasing magnetic field leads to a significant increase of the thermal width, and the thermal width in the case of dipole moving perpendicular to the magnetic field is apparently bigger than the case of dipole moving parallel to the magnetic field in the vicinity of the deconfined temperature ($T = 0.15$ GeV), which is consistent with Refs. [49,50]
(2) The thermal width in the case of the dipole moving parallel to the magnetic field is bigger than the case of dipole moving perpendicular to the magnetic field with $1.5T_c < T < 2T_c$.
(3) With the further increase of temperature ($T > 2T_c$), the thermal fluctuation becomes smaller and smaller.
(4) The effect of magnetic field on the thermal fluctuation is almost the same whether the dipole moves perpendicular or parallel to the magnetic field.

It is well known that the imaginary potential can be used to assess the thermal width of heavy quarkonium. It is argued that a large thermal width corresponds to a small dissociation length. Thus, the magnetic field has the effect of reducing the dissociation length or increasing the thermal width at the low deconfined temperature ($T = T_c = 0.15$ GeV). However, with the increase of temperature, the effect of magnetic field on thermal width and the dissociation length will gradually weaken.

Figure 7 shows the thermal width of the $\Upsilon(1S)$ with different rapidities and temperatures for the dipole moving parallel and perpendicular to the magnetic field case, respectively. It is found that the thermal width decreases with the increase of rapidity, which is in agreement with that computed by Refs. [32,51].

VI. CONCLUSION

The heavy-quark potential, whether it is a real potential or an imaginary potential, is very important quantity in gauge theories at finite temperature. It also has great relevance in connection with experimental programs in heavy-ion collisions at the RHIC and LHC energies. The melting of heavy quarkonia in a medium is considered to be one of the main experimental signatures for QGP formation. Current analyses of available research indicate that the matter formed in such collisions is strongly coupled. Thus, the study of the heavy-quark potential requires strong-coupling techniques, such as the AdS/CFT correspondence. There has been a lot of interest in the heavy-quarkonium suppression, which has been observed at the RHIC [1] and LHC [52,53]. The suppression is a signal of deconfinement, and it was suggested that the bound states dissociate in the hot thermal bath. It was proposed that the imaginary part of the potential $\mathrm{Im}V_{Q\bar{Q}}$ may be an important reason for this suppression rather than color screening.

By simulating the finite temperature and magnetic field at the RHIC and LHC energies of relativistic heavy-ion collisions, we restrict ourselves to the range of temperature and magnetic field corresponding to RHIC and LHC energy regions to study the potential and thermal width for the dipole moving parallel and perpendicular to the magnetic field. It is found that the magnetic field has less influence on the real potential but has greater influence on the imaginary potential. Extracting from the effect of thermal worldsheet fluctuations about the classical configuration, we investigate the thermal width of $\Upsilon(1S)$ in the

finite temperature magnetized background. The thermal width of $\Upsilon(1S)$ increases with the increasing magnetic field at the low deconfined temperature ($T_c = 0.15$ GeV), but with the increase of temperature ($T > 2T_c$), the thermal width hardly changes with the increase of magnetic field, which means the effect of high temperature completely exceeds that of magnetic field. The thermal width decreases with the increasing rapidity at the finite temperature magnetized background.

It is also found that the effect of a magnetic field on the thermal width when the dipole moves perpendicular to the magnetic field is larger than dipole moving parallel to the magnetic field at $T_c < T < 1.5T_c$, which implies that the magnetic field tends to enhance thermal fluctuation when dipole moves perpendicular to the magnetic field.

ACKNOWLEDGMENTS

This work was supported by National Natural Science Foundation of China (Grants No. 11875178, No. 11475068, and No. 11747115) and the CCNU-QLPL Innovation Fund (Grant No. QLPL2016P01).

[1] J. Adams *et al.* (STAR Collaboration), Nucl. Phys. **A757**, 102 (2005).
[2] K. Adcox *et al.* (PHENIX Collaboration), Nucl. Phys. **A757**, 184 (2005).
[3] E. V. Shuryak, Nucl. Phys. **A750**, 64 (2005).
[4] E. V. Shuryak, Phys. Rep. **61**, 71 (1980).
[5] T. Matsui and H. Satz, Phys. Lett. B **178**, 416 (1986).
[6] V. Skokov, A. Y. Illarionov, and V. Toneev, Int. J. Mod. Phys. A **24**, 5925 (2009).
[7] V. Voronyuk, V. D. Toneev, W. Cassing, E. L. Bratkovskaya, V. P. Konchakovski, and S. A. Voloshin, Phys. Rev. C **83**, 054911 (2011).
[8] A. Bzdak and V. Skokov, Phys. Lett. B **710**, 171 (2012).
[9] W. T. Deng and X. G. Huang, Phys. Rev. C **85**, 044907 (2012).
[10] Y. J. Mo, S. Q. Feng, and Y. F. Shi, Phys. Rev. C **88**, 024901 (2013).
[11] Y. Zhong, C. B. Yang, X. Cai, and S. Q. Feng, Adv. High Energy Phys. **2014**, 1 (2014).
[12] Y. Zhong, C. B. Yang, X. Cai, and S. Q. Feng, Chin. Phys. C **39**, 104105 (2015).
[13] D. She, S. Q. Feng, Y. Zhong, and Z. B. Yin, Eur. Phys. J. A **54**, 48 (2018).
[14] S. S. Gubser, I. R. Klebanov, and A. M. Polyakov, Phys. Lett. B **428**, 105 (1998).
[15] O. Aharony, S. S. Gubser, J. M. Maldacena, H. Ooguri, and Y. Oz, Phys. Rep. **323**, 183 (2000).
[16] M. Laine, J. High Energy Phys. 05 (2007) 028.
[17] P. Petreczky, C. Miao, and A. Mocsy, Nucl. Phys. **A855**, 125 (2011).
[18] N. Brambilla, M. A. Escobedo, J. Ghiglieri, J. Soto, and A. Vairo, J. High Energy Phys. 09 (2010) 038.
[19] Y. Burnier, M. Laine, and M. Vepsalainen, Phys. Lett. B **678**, 86 (2009).
[20] A. Rothkopf, T. Hatsuda, and S. Sasaki, Phys. Rev. Lett. **108**, 162001 (2012).
[21] M. Laine, O. Philipsen, P. Romatschke, and M. Tassler, J. High Energy Phys. 03 (2007) 054.
[22] A. Beraudo, J.-P. Blaizot, and C. Ratti, Nucl. Phys. **A806**, 312 (2008).
[23] N. Brambilla, J. Ghiglieri, A. Vairo, and P. Petreczky, Phys. Rev. D **78**, 014017 (2008).
[24] M. Á. Escobedo, J. Phys. Conf. Ser. **503**, 012026 (2014).
[25] A. Dumitru, Y. Guo, and M. Strickland, Phys. Rev. D **79**, 114003 (2009).
[26] M. Margotta, K. McCarty, C. McGahan, M. Strickland, and D. Yager-Elorriaga, Phys. Rev. D **83**, 105019 (2011); **84**, 069902(E) (2011).
[27] J. M. Maldacena, Int. J. Theor. Phys. **38**, 1113 (1999); Adv. Theor. Math. Phys. **2**, 231 (1998).
[28] J. Noronha and A. Dumitru, Phys. Rev. Lett. **103**, 152304 (2009).
[29] S. I. Finazzo and J. Noronha, J. High Energy Phys. 11 (2013) 042.
[30] K. Bitaghsir Fadafan, D. Giataganas, and H. Soltanpanahi, J. High Energy Phys. 11 (2013) 107.
[31] S. I. Finazzo and J. Noronha, J. High Energy Phys. 01 (2015) 051.
[32] M. Ali-Akbari, D. Giataganas, and Z. Rezaei, Phys. Rev. D **90**, 086001 (2014).
[33] Z. q. Zhang, D. F. Hou, and G. Chen, Phys. Lett. B **768**, 180 (2017).
[34] Z. q. Zhang and D. f. Hou, Phys. Lett. B **778**, 227 (2018).
[35] N. R. F. Braga and L. F. Ferreira, Phys. Rev. D **94**, 094019 (2016).
[36] J. Sadeghi and S. Tahery, J. High Energy Phys. 06 (2015) 204.
[37] A. V. Sadofyev and Y. Yin, J. High Energy Phys. 01 (2016) 052.
[38] T. Faulkner and H. Liu, Phys. Lett. B **673**, 161 (2009).
[39] H. Liu, K. Rajagopal, and U. A. Wiedemann, Phys. Rev. Lett. **98**, 182301 (2007).
[40] H. Liu, K. Rajagopal, and U. A. Wiedemann, J. High Energy Phys. 03 (2007) 066.
[41] Q. J. Ejaz, T. Faulkner, H. Liu, K. Rajagopal, and U. A. Wiedemann, J. High Energy Phys. 04 (2008) 089.
[42] K. A. Mamo, J. High Energy Phys. 05 (2015) 121.
[43] D. Dudal, D. R. Granado, and T. G. Mertens, Phys. Rev. D **93**, 125004 (2016).
[44] D. Li, M. Huang, Y. Yang, and P. H. Yuan, J. High Energy Phys. 02 (2017) 030.
[45] E. D'Hoker and P. Kraus, J. High Energy Phys. 10 (2009) 088.

[46] E. D'Hoker and P. Kraus, J. High Energy Phys. 03 (2010) 095.
[47] Z. R. Zhu, S. Q. Feng, Y. F. Shi, and Y. Zhong, Phys. Rev. D **99**, 126001 (2019).
[48] K. Bitaghsir Fadafan and S. K. Tabatabaei, J. Phys. G **43**, 095001 (2016).
[49] D. Dudal and T. G. Mertens, Phys. Rev. D **91**, 086002 (2015).
[50] N. R. F. Braga and L. F. Ferreira, Phys. Lett. B **783**, 186 (2018).
[51] M. A. Escobedo, J. Soto, and M. Mannarelli, Phys. Rev. D **84**, 016008 (2011).
[52] S. Chatrchyan *et al.* (CMS Collaboration), Phys. Rev. Lett. **109**, 222301 (2012); **120**, 199903(E) (2018).
[53] B. Abelev *et al.* (ALICE Collaboration), Phys. Rev. Lett. **109**, 072301 (2012).